Cation distribution in a Fe-bearing K-feldspar from Itrongay, Madagascar : a combined neutron- and X-ray single-crystal diffraction study

Autor(en): **Ackermann, Sonia / Kunz, Martin / Armbruster, Thomas**

Objekttyp: **Article**

Zeitschrift: **Schweizerische mineralogische und petrographische Mitteilungen = Bulletin suisse de minéralogie et pétrographie**

Band (Jahr): **84 (2004)**

Heft 3

PDF erstellt am: **27.04.2024**

Persistenter Link: https://doi.org/10.5169/seals-63754

Schweizerische Mineralogische und Petrographische Mitteilungen 84, 345–354, 2004

Cation distribution in a Fe-bearing K-feldspar from Itrongay, Madagascar: A combined neutron- and X-ray single-crystal diffraction study

Sonia Ackermann[1], *Martin Kunz*[2], *Thomas Armbruster*[3], *Jürg Schefer*[4] and *Henry Hänni*[5]

Abstract

We determined the cation distribution and ordering of Si, Al and Fe on the tetrahedral sites of a monoclinic low-sanidine from Itrongay, Madagascar, by combined neutron- and X-ray single-crystal diffraction. The cation distribution was determined by means of a simultaneous refinement using neutron- and X-ray data, as well as by combining scattering densities obtained from separate refinements with chemical data from a microprobe experiment. The two methods give the same results and show that Fe is fully ordered on T1, whereas Al shows a high degree of disorder. Based on this result and previously published temperature-dependent X-ray data, we conclude that it is preferential ordering of Fe on T1 even at high temperature, rather than high diffusion kinetics of Fe, which causes this asymmetry in ordering behaviour between Al and Fe. The preferential ordering of Fe relative to Al is in line with its 25 percent larger ionic radius.

Keywords: K-feldspars, single-crystal X-ray diffraction, neutron diffraction.

Introduction

K-feldspars (ideal formula $KAlSi_3O_8$) are classified as framework silicates. Their structure can be described as a framework of double-crankshaft chains parallel *a*, which in turn are formed by four-membered rings of $(Si,Al)O_4$ tetrahedra (Fig. 1). The silicate framework forms irregularly shaped cavities, which host the K ions (e.g. Ribbe, 1975; Smith 1974). K-feldspars are sub-divided according to their symmetry, which is mainly determined by ordering of Si and Al on the tetrahedral sites. In a unit cell of monoclinic feldspar, two symmetrically different tetrahedral sites (T1, T2) can be distinguished. High-sanidine as well as low-sanidine have monoclinic symmetry, where the only difference between these two minerals is the degree of ordering of Al and Si atoms on T1 and T2 (Smith, 1974). This is quantified through the parameter t1, which is defined as t1 = Al(T1) / [Al(T1) + Si(T1)]. K-feldspars formed at high temperature show a fully disordered distribution of Al and Si atoms over the two different T sites (t1 = 0.25). With increasing ordering, the Al atoms preferentially occupy the T1 site. K-feldspars have different mineral names assigned depending on the degree of ordering on T1 (Ribbe, 1975):

- high-sanidine: $0.25 < t1 < 0.333$ monoclinic
- low-sanidine: $0.334 < t1 < 0.37$ monoclinic
- orthoclase: $0.37 < t1 < 0.5$ monoclinic

Further ordering of Al and Si reduces the symmetry to triclinic thus creating four distinct tetrahedral sites (T1o, T1m, T2o, T2m). The triclinic polymorph is called microcline.

Fe-bearing K-feldspars from Itrongay, Madagascar, are known in the gem-industry for their golden coloured, transparent crystals up to several centimeters in size. A comprehensive review on the crystal chemistry of Itrongay K-feldspar is given by Blasi and De Pol Blasi (2000). The colouring of these gems is caused by a significant amount of Fe^{3+} substituting for Al^{3+}. Based on the amount of Fe^{3+} present and the assumption that Fe^{3+} adopts the same ordering scheme as Al^{3+}, a partial disorder of Fe^{3+} as found in orthoclase or low-sanidine was assumed for Itrongay K-feld-

[1] Department of Earth Sciences, University of Basel, Bernoullistr. 30, CH-4056 Basel, Switzerland.
[2] ALS, LBL, MS 4R 0230, 1 Cyclotron Rd, Berkeley CA 94720, USA; and Department of Earth and Planetary Sciences, University of California, Berkeley, CA-94720 USA. Corresponding author: <mkunz@lbl.gov>
[3] Laboratory for Chemical and Mineralogical Crystallography, University of Bern, Freiestrasse 3, CH-3012 Bern, Switzerland.
[4] Laboratory for Neutron Scattering, ETHZ and PSI, CH-5232 Villigen, Switzerland.
[5] Swiss Gemmological Institute, Falknerstrasse 9, CH-4001 Basel, Switzerland

0036-7699/04/0084/345

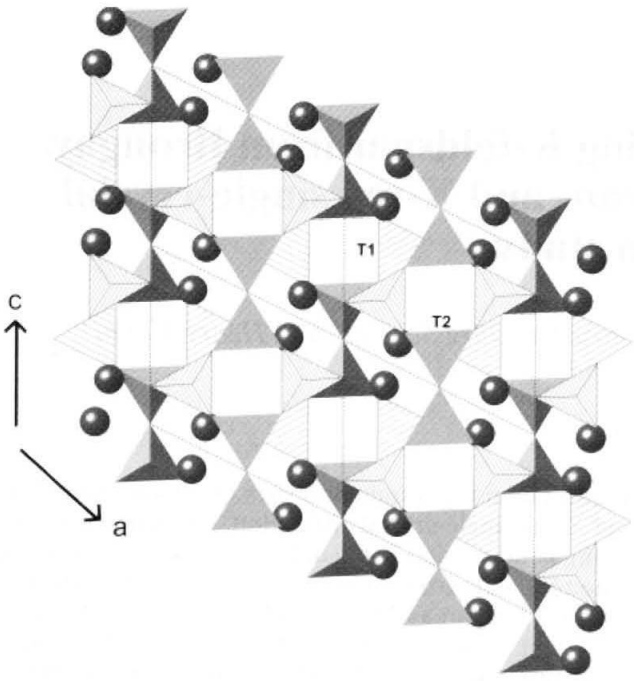

Fig. 1 Structural model of K-feldspar. A 3-dimensional framework of TO_4 tetrahedra (depicted as polyhedra) creates cavities, which host the large alkali cations (drawn as spheres). T1 (stripe-filled) and T2 (rendered gray) designate the two symmetrically distinguishable T-sites. Si, Al and Fe are distributed between these two sites in K-feldspar from Itrongay.

spars (Coombs, 1954; Hofmeister and Rossman, 1984). Optical investigations found that the incorporation of Fe^{3+} in K-feldspars leads to a change of the optical properties (shape, size and orientation of the optical indicatrix) when compared to Fe-free K-feldspars (Coombs, 1954; Walther, 1966). However, Behrens et al. (1995) propose on the basis of spectroscopic data that in their sample from Itrongay up to 50% of the Fe could be present in the form of sub-microscopic exsolution of a separate Fe-rich phase.

Gehring (1985) determined the Si–Al ordering characteristic for orthoclase using neutron single-crystal diffraction. He however did not take into account any Fe on the tetrahedral sites. A first experimental attempt to determine location and ordering pattern of Fe^{3+} in a K-feldspar was undertaken by Petrov and Hafner (1988) using electron paramagnetic resonance (EPR) on a sample from Volkesfeld (Eifel, Germany). They found Fe^{3+} to be disordered over T1 and T2 with a slight preference for T1. No quantitative measure of the degree of ordering is given. In contrast, Petrov et al. (1989) found with a similar EPR study that all Fe^{3+} was ordered onto the T1 site in albite ($NaAlSi_3O_8$).

Table 1 Neutron- and X-ray scattering lengths for elements relevant to Itrongay K-feldspar.

Atom	Neutron scattering length b ($\times 10^{-15}$ m) (Sears 1992)	X-ray scattering factor f_0 (electrons/atoms)
K	3.67	19
Na	3.63	11
Si	4.149	14
Al	3.449	13
Fe	9.54	26
O	5.803	8

A first attempt to determine the Fe-ordering in K-feldspar using diffraction methods was published by Kimata et al. (1996). Their refinement of T-site scattering-power led them to the conclusion that Fe was completely disordered over the available T-sites. However, they deduced the ordering based on <T–O> bond distances using a calibration gauged on Fe-free feldspars. More recently, Nyfeler et al. (1998) re-investigated a K-feldspar from Itrongay with X-ray techniques. A series of single-crystal X-ray diffraction experiments on annealed Itrongay specimens quenched from various temperatures and annealing times showed Fe^{3+} to be ordered on the T1 site (occ. Fe(T1) = 0.025, occ. Fe(T2) = 0), which is in contrast to the results of Kimata et al. (1996) and Petrov and Hafner (1988). Only at highest annealing temperatures and times a disordered distribution was observed (occ. Fe(T1) = 0.0125, occ. Fe(T2) = 0.0125). Nyfeler et al. (1998) determined the Si, Al, Fe distribution indirectly by comparing initial site assignments based on T–O bond length with the experimentally determined electron density. This was necessary, because a single diffraction experiment does not allow to unambiguously determine the concentration of three elements on a single site. For any given site, a single diffraction experiment provides one observed scattering density. Together with the requirement for full occupancy, this gives two known parameters, which is insufficient to derive three unknown occupancies. However, the use of bond lengths even for an initial estimate of the Si, Al distribution is also hampered by the fact that 5% Fe (ionic radius in tetrahedral coordination ~0.49 Å) can at least partially simulate the substitution of Al (ionic radius of Al in tetrahedral coordination ~0.39 Å) in a SiO_4 tetrahedron (ionic radius of Si in tetrahedral coordination ~0.26 Å) (Shannon, 1976). One possibility to unambiguously determine the distribution of three elements on a single site is to combine two diffraction experiments using two differ-

ent sets of scattering factors for the three elements in question. The combination of a neutron diffraction experiment and an X-ray diffraction experiment fulfils this condition, since the scattering factors for elastic diffraction are different for neutron- and X-ray-radiation, respectively (Table 1). Such an experiment gives two observable quantities (one X-ray scattering density, one neutron scattering density) for each site. These two observable parameters, combined with the crystal chemical condition that the total occupancy of each site has to be 1, gives a total of three observations to resolve the three unknown occupancy parameters on each T-site.

The most straightforward way to combine information of two different diffraction experiments is to refine the structural model simultaneously against both sets of diffraction data. While this is quite common for Rietveld refinement of powder diffraction data (e.g., Kunz et al., 1995), only one example is known to us where this has been applied to single-crystal diffraction data (Artioli et al., 1995). Here we present a simultaneous single-crystal structure refinement and compare its results to an 'external' determination of the cation distribution. For the 'external' procedure, X-ray and neutron data are used for separate refinements to extract average scattering densities for each radiation type at each T-site. This information is then combined with chemical information obtained from an electron microprobe experiment and the crystal chemical assumption of full occupancy for each site and a linear least-squares calculation is used to determine the cation distribution, which fits all observable quantities.

Experimental methods

The single-crystal sample from Itrongay Madagascar is of gemstone quality in terms of clarity and colour (pale golden). For the neutron diffraction experiment, the single crystal was shaped to an optically perfect sphere of 10 mm in diameter. Small fractions of the same single crystal were prepared for the X-ray scattering experiment, as well as for the microprobe analysis.

Electron microprobe

For chemical analysis, the electron microprobe JEOL JXA 8600 of the Institute of Mineralogy and Petrology of the University of Basel, Switzerland, was used. An accelerating voltage of 15 kV together with a sample current of 10 nA were used as operating conditions. A defocused beam (5 μm) was used in order to avoid loss of K atoms in the electron beam. Graphtonite for Fe, orthoclase ($KAlSi_3O_8$) for K and Al, albite ($NaAlSi_3O_8$) for Na and Si were used as standards. The homogeneity of the crystal was tested with a line scan covering the whole crystal with 20 single-spot measurements. The average of the 20 individual measurements was assumed to represent the chemical composition. Standard deviations given in the chemical formula refer to the scatter of the 20 individual measurements.

X-ray data collection

X-ray data collection of the Madagascar K-feldspar was performed at room temperature on an Enraf-Nonius CAD4 single-crystal diffractome-

Table 2 Experimental details for X-ray and Neutron data collection.

	X-ray	Neutrons
Crystal size	290×220×190 μm	10mm
Diffractometer	Enraf-Nonius CAD 4	TriCS
Wavelength	0.7071 Å	1.18 Å
a (Å)	8.5832 (7)	8.5992 (4)
b (Å)	13.0076 (9)	13.0277 (8)
c (Å)	7.1943 (6)	7.1926 (6)
β (°)	116.023 (6)	116.056 (6)
V (Å^3)	721.8 (1)	723.9 (1)
Absorption correction	Psi scan	none
Maximum $\sin\theta/\lambda$	0.9	0.6
Measured reflections	2856	1183
Index range	$-15 \leq h \leq 14$	$-7 \leq h \leq 10$
	$-1 \leq k \leq 23$	$-10 \leq k \leq 14$
	$-1 \leq l \leq 12$	$-8 \leq l \leq 4$
Unique reflections	2302	483
Refl. > 4σ (Fo) read by ShelxL	2023	483
Refl. > 3σ (Fo) read by GSAS:	2646	853

Table 3 Refinement details for X-ray and neutron data.

	SHELX X-ray	SHELX Neutrons	GSAS
R_{int}	0.012	0.043	0.028 / 0.046[1)]
Number of variables	55	55	71
R1, Fo>4σ (Fo) (3σ (Fo) for GSAS)	0.0210[2)]	0.0493[2)]	0.040[1)]
R1 all data	0.0264[2)]	0.0490[2)]	n/a
wR2 (on Fo^2)	0.0631[3)]	0.1202[3)]	0.040[4)]
Extinction parameters[5)]	x = 0.021 (2)	x = 1.08 (8)	X-rays: $E_g = 7.6(1)\ 10^5$ $E_s = 7.9(1)\ 10^{16}$ Neutr.: $E_g = 2.09(3)\ 10^{-3}$ $E_s = 2.1(1)\ 10^{-5}$

[1)] $R=(\Sigma|Fo^2-SFc^2|)/(\Sigma|Fo^2|)$, where S is the scale factor.
[2)] $R1 = (\Sigma||F_{obs}| - |F_{calc}||)/(\Sigma|Fobs|)$.
[3)] $wR2 = \{\Sigma[w(F_{obs}^2 - F_{calc}^2)^2]/\Sigma[w(F_{obs}^2)^2]\}^{1/2}$, where $w = [\Sigma^2(Fobs^2)+(aP)^2+bP]^{-1}$, and $P = [2F^2_{calc} + Max(F_{obs}^2,0)]/3$.
[4)] In GSAS: $Rw=[\Sigma w(Fo^2-SFc^2)^2/(\Sigma w|Fo^2|)]$.
[5)] SHELX: F_c is multiplied by $k[1+0.001xF_c^2\lambda^3/\sin(2\theta)]^{-1/4}$; x is refined.
GSAS: F_c^2 is divided by $E_h = \{1+2x+[0.58+0.48\cos(2\theta)+0.24\cos^2(2\theta))x2]/[1+(0.02-0.025\cos(2\theta)x]\}^{1/2}$.
x for X-rays: $[7.9406\times10^5\ \lambda^2F_c^2E_g(\cos(2\theta_M)+\cos^4(2\theta)]/[V_o^2(\cos(2\theta_M+\cos^2(2\theta))(1+(E_s\sin(2\theta)/\lambda E_G^2))^{1/2}]$;
x for neutrons: $[1.0\times10^7\ \lambda^2F_c^2\times E_g]/\ V_o^2\ (1+(E_s\times\sin(2\theta)/\lambda\times E_G^2))^{1/2}]$,
E_g and E_s, accounting for Gaussian contributions of secondary extinction type I and II, respectively, are refined.

ter at the Laboratory for Chemical and Mineralogical Crystallography in Bern using graphite monochromatized MoKα radiation. Data were recorded with a single point detector using omega–theta scans. Cell dimensions were refined from the angular settings of 22 reflections with $23° < \theta < 28°$. An empirical absorption correction using the Ψ-scan technique was applied. Data reduction as well as Lorentz and polarisation corrections were performed with the SDP program package (Enraf-Nonius, 1983). Additional experimental details are summarized in Tables 2 and 3.

Neutron data collection

The neutron-diffraction experiment was performed on the single-crystal diffractometer TriCS at the Swiss Spallation Source SINQ at Paul Scherrer Institute, Switzerland, using a single tube detector. Cell dimensions were refined from the angular settings of 15 reflections with $7°< \theta < 47°$ Data reduction was performed using the program Rafin/ILL. Data reduction was done using trics_ccd / PSI. A set of 1183 reflections was measured over the period of 5 days. Due to the spherical shape of the sample a correction for anisotropic absorption was not necessary. Additional experimental details are summarized in Tables 2 and 3.

Structure refinement

We attempted to resolve the Si, Al, Fe distribution on T1 and T2 by simultaneously refining the structural model against the X-ray and neutron data sets, respectively. This was done using the program package GSAS (Larsen and Von Dreele, 2000; Toby, 2001), which, to the best of our knowledge, is the only structure refinement package that allows use of two single-crystal diffraction data sets simultaneously. The validity of this method was crosschecked by separate refinements in Shelxl97 (Sheldrick, 1997) using the same data and combining those results with chemical data from the electron-microprobe experiment.

When simultaneously refining a structural model against X-ray and neutron data, two difficulties need to be addressed:

(1) The occupancy of the T-sites needs to be constrained such that its total value does not exceed one. This is not straightforward in GSAS when constraining three different cations on one site, since GSAS allows constraining relative shifts of a given variable rather than a target value. The target value, i.e. in our case the total occupancy of a given site is determined when entering the starting values. By constraining the relative shifts correctly, one is able to ensure that the cation sum stays at the desired value, while the relative contributions of the individual cations are allowed to change. In order for this to be applicable, an even number of cation-species has to be refined for a given site (Joubert et al., 1998). Therefore, in the case of three cation species on a single site, one of the cation-species needs to be doubled with all atomic parameters except the occupancy constrained to be equal. In our example, for each T-site we create four sites, one for Si, one for Al and

Table 4 Atomic coordinates, occupancy and U_{eq} as derived from GSAS refinement using X-ray and neutron single-crystal data simultaneously.

Atom	x	y	z	occupancy	U_{eq} (Å^2)
K	0.21471 (7)	1/2	0.3619 (1)	0.895 (5)	0.0270 (3)
Na	0.21471 (7)	1/2	0.3619 (1)	0.105 (5)	0.0270 (3)
Si T1				0.65 (2)	0.0107 (2)
Al T1	0.99057 (5)	0.18506 (3)	0.27623 (6)	0.33 (2)	0.0107 (2)
Fe T1				0.02 (2)	0.0107 (2)
Si T2				0.88 (2)	0.0105 (2)
Al T2	0.20953 (5)	0.38208 (3)	0.84432 (6)	0.12 (2)	0.0105 (2)
Fe T2				0.00 (2)	0.0105 (2)
O1	0.1382 (1)	1/2	0.7850 (1)	1.0	0.0207 (5)
O2	0.31989 (8)	0.37375 (4)	0.09434 (9)	1.0	0.0201 (3)
O3	0	0.14652 (6)	1/2	1.0	0.0210 (5)
O4	0.03536 (8)	0.31106 (4)	0.7585 (1)	1.0	0.0193 (3)
O5	0.17230 (8)	0.14693 (4)	0.2726 (1)	1.0	0.0252 (4)

two for Fe, where all positional parameters as well as displacement parameters are constrained to be equal and the initial occupancies of these four sites are chosen such that its sum is one. During the refinement, the shifts of the occupancies for these four sites can then be constrained pair-wise, such that the total sum of the cations stays at the initial value of one. The sum of the occupation of the two Fe-sites represents the total Fe-occupation on the T-site in question. We thus introduced two constrains for each of the two T-sites:

Shift (Si) = –Shift (Fe1)
Shift (Al) = –Shift (Fe2)

(2) The extinction process of an incident beam in a single crystal is different for X-rays and for neutrons. This difference is mainly due to the stronger penetration depth (lower absorption) and thus mosaic sampling of neutrons (Bacon, 1955). This fact is accounted for by GSAS in that it employs a different formalism to correct for extinction in the case of neutrons and X-rays, respectively (Larsen and Von Dreele, 2000; p. 128–129). However, GSAS does not allow refinement of two different extinction parameters for the two different datasets used simultaneously in our refinement. In order to circumvent this problem, two crystals ('phases' in GSAS terminology) have to be introduced into the refinement, where of course all atomic parameters of the two 'phases' are mutually constrained to be equal. One of the 'phases' is assigned to the X-ray data-set and the second 'phase' to the neutron data-set, thus allowing refinement of separate extinction parameters for the two data-sets. We refined parameters for a Gaussian approximation for combined secondary extinction types I and II for both phases (Table 3).

Constraining three cation species onto the T-sites and refining a separate extinction parameter for the two datasets resulted in a total of 88 constraints. Anisotropic displacement parameters (U_{ij}) and occupation parameters were varied in alternating cycles and left free simultaneously in the very last cycles. This is justified since the simultaneous use of neutron and X-ray data strongly diminishes the correlation between occupancies and displacement parameters in the non-linear least squares procedure (Artioli et al., 1995). Scattering factors for neutral atoms were used for cations as well as anions. A combined Lorentz-Polarisation correction was also applied.

To assess the reliability of the above described simultaneous refinement, a second procedure to extract the cation distribution which includes chemical information, was adopted: Two separate refinements for the X-ray and the neutron data set, respectively, were performed using the program package SHELXL (Sheldrick, 1997). When doing this, each T-site is introduced only once and assigned a dummy Si-atom. The refined occupancy for this dummy atom allows deducing the average scattering density by multiplying it with the respective scattering power (14 for Si in the case of X-rays, 4.149 in the case of neutrons, see Table 1) of the dummy atom. This refinement procedure thus extracts two scattering densities (one for X-rays, one for neutrons) for each T-site. When using one data set at a time, occupancy parameters and displacement parameters cannot be refined simultaneously due to their high correlation (e.g. Armbruster et al., 1990). It turns out that the final values of displacement parameters and occupancies are biased by the starting values, even if occupancies and displacement parameters are fixed in alternating cycles during the refinement. In order to avoid this bias, we fixed the displacement para-

meters of the tetrahedral sites at the values retrieved from the simultaneous refinement, where this correlation is suppressed.

The scattering densities for the tetrahedral sites obtained by this way are supplemented by the chemical information from the microprobe analysis (i.e. the total amount of Si, Al, and Fe atoms for both T-sites) together with the crystal chemical constraint that each of the two T-sites has to be fully occupied. This results in a total of 9 observations to deduce 6 variables. Since all 9 equations are linear, a linear least-squares calculation can be employed to calculate the cation distribution best complying with the different observations. These calculations were done in MS Excel. Table 3 summarizes further details for the structural refinements.

Results

The chemical analysis by electron microprobe gave a composition of $K_{1.03(2)}$ $Na_{0.056(3)}$ $Fe_{0.046(4)}$ $Al_{0.87(1)}$ $Si_{3.04(2)}O_8$. The composition agrees well with the value obtained from the structure refinement except for the akali cations. The excess alkali content is striking but seems to be consistent through the entire crystal. One possible explanation is Na-volatilisation in the albite standard. We do not believe that this aberration is an indication for any submicroscopic exsolution of a Fe-rich phase, as observed by Behrens et al. (1995), since it is difficult to conceive a mechanism where an undetected Fe-oxide is reflected in an excess alkali content. Also, the crystals investigated are very clear with no indications of exsolution or inclu-

Table 5 Anisotropic displacement parameters (Å²) as derived from GSAS refinement using X-ray and Neutron single-crystal data simultaneously.

Atom	U_{11}	U_{22}	U_{33}	U_{12}	U_{13}	U_{23}
K / Na	0.0177 (2)	0.0334 (3)	0.0270 (3)	0	0.0070 (2)	0
T1	0.0114 (2)	0.0118 (2)	0.0092 (2)	0.0022 (1)	0.0047 (1)	0.0011 (1)
T2	0.0110 (2)	0.0093 (2)	0.0107 (2)	0.0002 (1)	0.0042 (1)	–0.0001 (1)
O1	0.0206 (5)	0.0136 (4)	0.0205 (5)	0	0.0021 (4)	0
O2	0.0221 (4)	0.0210 (3)	0.0116 (3)	0.0023 (2)	0.0022 (3)	0.0017 (2)
O3	0.0249 (5)	0.0211 (4)	0.0173 (5)	0	0.0093 (4)	0
O4	0.0184 (3)	0.0180 (3)	0.0195 (3)	–0.0027 (2)	0.0063 (3)	–0.0033 (3)
O5	0.0231 (4)	0.0328 (4)	0.0244 (4)	0.0044 (3)	0.0146 (3)	–0.0007 (3)

Table 6 Atomic coordinates, Population and U_{eq} as derived from SHELX refinement using X-ray and neutron single-crystal data separately. The occupation of the T-sites refers to a hypothetical dummy Si-atom placed on the T-site. U_{eq} for A cations and T-sites were fixed at values derived from GSAS.

X-rays:

Atom	x	y	z	Occupancy	U_{eq} (Å²)
K	0.21490 (4)	1/2	0.36215 (5)	0.91 (2)	0.027
Na	0.21490 (4)	1/2	0.36215 (5)	0.09 (2)	0.027
T1 (Si)	0.99056 (3)	0.18503 (2)	0.27617 (3)	0.957 (1)	0.0107
T2 (Si)	0.20946 (2)	0.38211 (1)	0.84437 (3)	0.968 (1)	0.0107
O1	0.1376 (1)	1/2	0.7847 (2)	1.0	0.0222 (6)
O2	0.31960 (8)	0.37380 (5)	0.09451 (9)	1.0	0.0203 (4)
O3	0	0.14630 (7)	1/2	1.0	0.0214 (6)
O4	0.03516 (8)	0.31119 (5)	0.7585 (1)	1.0	0.0193 (4)
O5	0.17233 (9)	0.14676 (6)	0.2730 (1)	1.0	0.0257 (5)

Neutrons:

Atom	x	y	z	Occupancy	U_{eq} (Å²)
K	0.2146 (5)	1/2	0.3624 (6)	1.01 (2)[1)]	0.027
T1 (Si)	0.9904 (2)	0.1851 (1)	0.2758 (3)	0.994 (5)	0.0107
T2 (Si)	0.2100 (2)	0.3820 (3)	0.8443 (3)	1.000 (5)	0.0107
O1	0.1386 (3)	1/2	0.7858 (3)	1.0	0.020 (1)
O2	0.3199 (2)	0.3738 (1)	0.0943 (2)	1.0	0.018 (1)
O3	0	0.1463 (1)	1/2	1.0	0.024 (1)
O4	0.0355 (2)	0.31105 (9)	0.7588 (2)	1.0	0.017 (1)
O5	0.1724 (2)	0.1470 (1)	0.2727 (2)	1.0	0.020 (1)

[1)] Na and K cannot be distinguished with neutron radiation (Table 1)

sions. In any case, we believe this to be due to some unexplained experimental artefact, rather than a real chemical feature

Cell parameters

As can be seen on Table 2, cell parameters retrieved from the X-ray and neutron diffraction experiment differ significantly. This discrepancy cannot only be attributed to a remaining uncertainty in the exact wavelength of the neutron radiation, since the shift is different for the three axes. However, results concerning lattice constants from single-crystal neutron data are limited by the large size of the crystal. The values from the X-ray experiment agree well with previously determined unit cells and are thus used for the bond-length calculations.

Simultaneous refinement

Fractional coordinates, occupation parameters and isotropic displacement parameters are listed in Table 4. Table 5 reports the anisotropic displacement parameters. Assigning the Fe-occupancy is complicated because of the very low total Fe-content. Although the refinement assigns all Fe to T1, this value is still only one estimated standard deviation (esd) above zero. However, this result is obtained consistently from different starting values. This seems to suggest a strong tendency for ordering of Fe on T1, while Al shows some degree of disorder. Using t1 to quantify the ordering of Al on the T1 site we obtain t1 = 0.34(2). The A site refined to an occupancy of 90% K and 10% Na. Converting the refined site occupancies into a chemical formula yields

$K_{0.895(5)}Na_{0.105(5)}Fe_{0\cdot04(4)}Al_{0.90(4)}Si_{3.06(4)}O_8$, which matches the results obtained from the electron microprobe

$(K_{1.03(2)}\ Na_{0.056(3)}\ Fe_{0.046(4)}\ Al_{0.87(1)}\ Si_{3.04(2)}O_8)$ well, except for the problematic alkali cations (see above). The Fe/Si/Al ratio derived from structural refinement is identical within experimental uncertainties to the composition found by Kimata et al. (1996).

Table 7 Anisotropic displacement parameters (Å^2) as derived from SHELX refinements. The values of the T-sites were set to the values obtained from the simultaneous refinement.

X-rays:

Atom	U_{11}	U_{22}	U_{33}	U_{12}	U_{13}	U_{23}
K / Na	0.0155 (3)	0.0308 (4)	0.0252 (3)	0	0.0061 (2)	0
O1	0.0203 (7)	0.0131(6)	0.0241 (8)	0	0.0034 (6)	0
O2	0.0211 (5)	0.0208 (5)	0.0136 (4)	0.0020 (4)	0.0029 (4)	0.0016 (4)
O3	0.0254 (8)	0.0204 (8)	0.0191 (7)	0	0.0105 (6)	0
O4	0.0171 (5)	0.0173 (5)	0.0221 (5)	–0.0020 (4)	0.0067 (4)	–0.0025 (4)
O5	0.0219 (6)	0.0325 (7)	0.0262 (6)	0.0037 (5)	0.0150 (5)	–0.0007 (5)

Neutrons:

Atom	U_{11}	U_{22}	U_{33}	U_{12}	U_{13}	U_{23}
K	0.026 (5)	0.035 (3)	0.032 (4)	0	0.015 (4)	0
O1	0.019 (3)	0.012 (2)	0.018 (3)	0	0.002 (3)	0
O2	0.020 (2)	0.018 (1)	0.010 (2)	0.002 (1)	0.003 (2)	0.001 (1)
O3	0.024 (3)	0.019 (2)	0.014 (2)	0	0.009 (2)	0
O4	0.017 (2)	0.015 (1)	0.017 (2)	–0.002 (1)	0.005 (2)	–0.003 (1)
O5	0.022 (2)	0.030 (2)	0.022 (2)	0.004 (1)	0.014 (2)	–0.000(1)

Table 8 Observed and calculated values from the linear least-squares calculation to obtain the cation distribution.

	Observed	Calculated
Average neutron scattering density on T1 (fm)	4.123 (4)	4.034 (30)
Average X-ray scattering density on T1 (electrons/atom)	13.39 (1)	13.62 (3)
Average neutron scattering density on T2 (fm)	4.149 (4)	4.053 (30)
Average X-ray scattering density on T2 (electrons/atom)	13.552 (1)	13.829 (30)
Total occupancy T1	1	0.998 (30)
Total occupancy T2	1	0.996 (30)
Total Si p.f.u	3.04 (2)	3.07 (3)
Total Al p.f.u	0.87 (1)	0.87 (3)
Total Fe p.f.u	0.046 (4)	0.05 (3)

Separate refinement

Fractional coordinates, occupancy parameters and isotropic displacement parameters are given in Tables 6. Table 7 lists the anisotropic displacement parameters of the A-cation and oxygen atoms. The displacement parameters of the T-sites were fixed at the values obtained from the combined refinement (Table 5) (see above). The combined data together with the assumption of full occupancy allows solving the linear least squares problem of the cation distribution. A diagonal matrix with the squares of the experimental standard deviations was used as the variance matrix, which helped to estimate uncertainties of the linear least-squares calculation. Table 8 shows the agreement between observed and calculated values of the linear least-squares calculation.

Discussion

The three different refinements gave consistent results in terms of atomic coordinates and anisotropic displacement parameters (ADP's) (Tables 4–7). For the ADP's, most values are identical within 2 standard deviations. For the coordinates, the scatter is ~3 standard deviations. The biggest differences are observed between the separate refinement using neutron data only on one hand and the X-ray refinement and simultaneous refinement on the other hand. We attribute this to the rather low number of unique observations in the neutron data set. The T–O bond lengths derived from these coordinates show a larger average value for T1 compared to T2 (Table 9). These values are in excellent agreement with the average T–O bond lengths reported by Nyfeler et al (1998). The observed asymmetry in <T–O> is in accordance with a higher occupancy of larger cations on T1. Although it is not possible to uniquely deduce the cation distribution of three cations from the bond lengths alone, we can in turn deduce an expected average bond length from our refined cation distribution. This can be done by using end-member bond lengths for Si–O (1.61 Å), Al–O (1.75 Å) and Fe^{3+}–O (1.84 Å) as given by Shannon (1976). The average bond length of a site, which in spatial average is occupied by several cations, can then be deduced as an average of these end-member bond lengths weighted with the appropriate cation concentration (Virials theorem). If we use the T-occupancies as obtained from the simultaneous refinement (GSAS) we obtain expected average <T–O> bond lengths of 1.660 (5) Å and 1.626 (5) Å for T1 and T2 respectively. This matches the observed values of 1.655 (1) Å and 1.629 (1) Å (Table 9) quite well, thus giving further credibility to our refined cation distribution.

Table 9 T–O bond lengths (Å) derived from the simultaneous refinement using GSAS.

T1:	
O2	1.6618 (7)
O3	1.6538 (5)
O4	1.6581 (6)
O5	1.6479 (7)
<T1 – O>	1.655 (1)
T2:	
O1	1.6372 (5)
O2	1.6277 (7)
O4	1.6308 (7)
O5	1.6209 (6)
<T2 – O >	1.629 (1)

The cation distribution obtained by the simultaneous refinement is further supported when comparing them with the result obtained from the separate refinement (Table 10). The results of the two methods are identical within one sigma. They also confirm the finding of Nyfeler et al. (1998), and show that Fe^{3+} cations are preferentially ordered on the T1 sites in K-feldspar of Itrongay. Iron thus shows a very high degree of ordering in the K-feldspar structure, in contrast to the rather high degree of disorder observed of Al. However,

Table 10 Comparison between cation distribution as obtained from a simultaneous refinement against X-ray- and neutron-data (left) and from a linear least-squares calculation using separate scattering densities plus chemical data (right). See text for details.

	occupancies from simultaneous refinement	occupancies from separate refinement
T1 Si	0.65 (2)	0.65 (3)
T1 Al	0.33 (2)	0.32 (3)
T1 Fe	0.02 (2)	0.023(9)
T2 Si	0.88 (2)	0.88 (3)
T2 Al	0.12 (2)	0.113 (9)
T2 Fe	0.00 (2)	0.000 (2)

our results of site occupancies for a Fe-bearing K-feldspar are in disagreement with the derived ordering scheme found by Petrov and Hafner (1988). They suggest a highly disordered distribution of Fe atoms over the two T sites. As a result, the authors concluded slower kinetics for Fe^{3+} diffusion than for all the other diffusion processes in the crystal structure. It is difficult to interpret our finding of high Fe-ordering in K-feldspar in terms of diffusion kinetics in the absence of temperature dependent data. The high degree of Fe-ordering can be caused either by very rapid diffusion and thus ordering of Fe^{3+} cations during fast cooling or by a much stronger site preference of Fe^{3+} for T1, which would force Fe^{3+} to be ordered onto T1 even at highest temperatures. In order to properly assess the kinetics of tetrahedral cation diffusion with diffraction methods, simultaneous X-ray and neutron data at various elevated temperatures would be needed. Unfortunately, this is rather difficult in view of limited experimental time available at neutron sources.

However, in view of the results of Nyfeler et al. (1998) and its agreement with our present study, the interpretation of a crystal chemical preference for the T1 site rather than a faster diffusion kinetics of Fe^{3+} seems likely: For equivalent quenching times, a slight increase in Fe-disorder was deduced for samples, which had been annealed for long times at high temperatures, relative to samples annealed only shortly at equivalent temperatures. This would not be expected, if it were the faster diffusion during the quenching process, which causes the high degree of Fe-ordering. A stronger ordering of Fe^{3+} relative to Al^{3+} in T1 is also consistent with its 25 percent larger ionic radius.

In conclusion, we find that simultaneous refinement of a structural model against X-ray and neutron data is a fast and reliable tool not only when using powder data, but also for single-crystal diffraction data. In mineralogy, the problem of determining the distribution of various elements on a given site is frequently encountered. It would therefore be desirable that this option is exploited more in other refinement packages.

Our combined X-ray and neutron study on Itrongay K-feldspar confirmed the cation distribution proposed by Nyfeler et al. (1998) on the basis of X-ray data only. It is in disagreement with an earlier EPS study (Petrov and Hafner, 1988) and a diffraction study of Kimata et al. (1996). Given the robustness of a combined X-ray/neutron diffraction experiment, this result should help clarify on the debate on ordering of Fe within the tetrahedral framework of feldspar (Blasi and De Pol Blasi, 2000). The increase in ordering with increasing ionic radius along the series Si, Al, Fe suggests that ordering in silicate frameworks is primarily driven by ionic size. It is thus to be expected that other impurities would follow this pattern, i.e. Ti^{4+} (ionic radius = 0.42 Å), if present in tetrahedral coordination, would behave similar to Al^{3+} (ionic radius = 0.39 Å), while possible P^{5+} impurities (ionic radius = 0.17 Å) would show even lower preference for T1 than Si (ionic radius = 0.26 Å).

Acknowledgements

This work was partially performed at TriCS / SINQ at the Paul Scherrer Institute in Villigen, Switzerland, Proposal Number II / 03 S-5. Martin Kunz is supported by COMPRES, the Consortium for Materials Properties Research in Earth Sciences under NSF Cooperative Agreement EAR 01-35554. Thomas Armbruster acknowledges support from the 'Schweizerische Nationalfonds'. We thank Kathy Waite for her help during microprobe analysis and Drs. Achille Blasi (Università di Milano), Andrew C. McCarthy (University of Arizona), and Joe R. Smyth (University of Colorado) for their constructive reviews. The submitted manuscript has been co-authored by a contractor of the U.S. Government under contract No. DE-AC03-76SF00098. Accordingly, the U.S. Government retains a nonexclusive royalty-free license to publish or reproduce the published form of this contribution, or allow others to do so, for U.S. Government purposes.

References

Armbruster, T., Bürgi, H.-B., Kunz, M., Gnos, E., Brönnimann, S. and Lienert, C. (1990): Variation of displacement parameters in structure refinements of low albite. *Am. Mineral.* **75**, 135–140.

Artioli, G., Rinaldi, R., Wilson, C.C. and Zanazzi, P.F. (1995): Single-crystal pulsed neutron diffraction of a highly hydrous beryl. *Acta Cryst.* **B51**, 733–737.

Coombs, D.S. (1954): Ferriferous orthoclase from Madagascar. *Mineral. Mag.* **30**, 409–427.

Bacon, G.E. (1955): Neutron Diffraction. Oxford University Press, London. 51 pp.

Behrens, H.U., Krause, C. and Kroll, H. (1995): TEM-investigation of the sanidine/microcline transition across metamorphic zones: the K-feldspar varieties. *Eur. J. Mineral.* **1**, 47–58.

Blasi, A. and DePol Blasi, C. (2000): Crystal structures of alkali feldspars from granitic pegmatites: A review. *Memorie della Societa Italiana di Scienza Naturali e del Museo Civico di Storia Naturale, Milano* **Vol. XXX**, 73–109.

Enraf Nonius (1983): Structure Determination package (SDP) Enraf-Nonius. Delft, Netherlands.

Gehring, E. (1985): Silizium/Aluminium-Ordnung und Kristallperfektion von Sanidinen. Ph.D. Dissertation, Institut für nukleare Festkörperphysik, Kernforschungszentrum, Karlsruhe, unpubl.

Hofmeister, A.M. and Rossman, G.R. (1984): Determination of Fe^{2+} and Fe^{3+} concentrations in feldspar by optical absorption and EPR spectroscopy. *Phys. Chem. Min.* **11**, 213–224.

Joubert, J.M., Cerny, R., Latroche, M. Percheron-Guegan, A. and Yvon, K. (1998): Site occupancies in the battery electrode material $LaNi_{3.55}Mn_{0.4}Al_{0.3}Co_{0.75}$ as

determined by multiwavelength synchrotron powder diffraction. *J. Appl. Cryst.* **31**, 327–332.

Kimata, M., Saito, S., Shimizu, M., Iida, I. and Matsui, T. (1996): Low-temperature crystal structures of orthoclase and sanidine. *Neues Jahrbuch für Mineralogie Abhandlungen* **171**, 199–213.

Kunz, M., Dinnebier, R., Cheng, L.K., McCarron III, E.M., Cox, D.E., Parise, J.B., Gehrke, M., Calabrese, J., Stephens, P.W., Vogt, T. and Papoular, R. (1995): $Cs(TiAs)O_5$ and $Cs(TiP)O_5$: A disordered parent structure of $ABOCO_4$ compounds. *J. Sol. State Chem.* **120**, 299–310.

Larson, A.C. and Von Dreele, R.B. (2000): General Structure Analysis System (GSAS), Los Alamos National Laboratory Report LAUR 86–748.

Nyfeler, D., Armbruster, T. and Villa, I. M. (1998): Si, Al, Fe order disorder in Fe bearing K-feldspars from Madagascar and its implication on Ar diffusion. *Schweiz. Mineral. Petrogr. Mitt.* **78**, 11–20.

Petrov, I. and Hafner, S.S. (1988): Location of trace Fe^{3+} ions in sanidine, $KAlSi_3O_8$. *Am. Mineral.* **73**, 97–104.

Petrov, I., Yude, F., Bershov, L.V., Hafner, S.S. and Kroll, H. (1989): Order-disorder of Fe^{3+} ions over the tetrahedral positions in albite. *Am. Mineral.* **74**, 604–609.

Ribbe, P.H. (1975): Feldspar Mineralogy. *Mineralogical Reviews* **Vol. 2**, Mineralogical Society of America, Washington.

Sears, V.F. (1992): Neutron scattering length and cross section. *Neutron News* **3(3)**, 26–37.

Shannon, R.D. (1976): Revised effective ionic radii and systematic studies of interatomic distances in halides and chalcogenides. *Acta Cryst.* **A 32**, 751.

Sheldrick, G.M. (1997): SHELXL-97-A program for crystal structure refinement. University of Göttingen, Germany, Release 97-2.

Smith, J.V. (1974): Feldspar Minerals, Springer-Verlag, Göttingen.

Toby, B.H. (2001): EXPGUI, a graphical user interface for GSAS. *J. Appl. Cryst.* **34**, 210–213.

Walther, V. (1966): Der Orthoklas von Itrongay auf Madagaskar und seine Einordnung in das System der Kalifeldspäte. Ph.D. dissertation. Universität Hamburg, unpubl.

Received 20 December 2004
Accepted in revised form 2 May 2005
Editorial handling: R. Gieré